frontiers | Frontiers in Earth Science

TYPE Original Research
PUBLISHED 22 January 2024
DOI 10.3389/feart.2024.1340523

OPEN ACCESS

EDITED BY
Maxim Lebedev,
Edith Cowan University, Australia

REVIEWED BY
Haihai Hou,
Liaoning Technical University, China
Qian Zhang,
Peking University, China
Longyi Shao,
China University of Mining and Technology, Beijing, China

*CORRESPONDENCE
Ruikang Cui,
ruikang_cui@163.com

RECEIVED 18 November 2023
ACCEPTED 08 January 2024
PUBLISHED 22 January 2024

CITATION
Shi Y, He Y, Wan J, Sun J, Zeng J and Cui R (2024), The primary controlling factors of the occurrence state of deep high-rank coalbed methane in eastern Ordos Basin.
Front. Earth Sci. 12:1340523.
doi: 10.3389/feart.2024.1340523

The primary controlling factors of the occurrence state of deep high-rank coalbed methane in eastern Ordos Basin

Yujiang Shi[1], Yufei He[1], Jinbin Wan[1], Jianmeng Sun[2], Jingbo Zeng[1] and Ruikang Cui[2]*

[1]China National Logging Corporation, Xi'an, Shaanxi, China, [2]School of Geosciences, China University of Petroleum (East China), Qingdao, China

Introduction: This study investigates the key controlling factors of the occurrence state of deep coalbed methane (CBM). CBM is an abundant energy resource in China, particularly in deep coal seams. However, the exploration and development of deep CBM face numerous challenges, and the understanding of the controlling factors of its occurrence state is still limited.

Methods: The study reveals that deep CBM primarily exists in the form of adsorbed gas and free gas within the pore-fracture system of coal. Factors such as formation temperature, formation pressure, pore structure, and water saturation collectively influence the occurrence state of deep CBM. By employing the Simplified Local Density (SLD) model and molecular simulation methods.

Results and discussion: This study examines the impact of two external geological control factors (formation temperature, formation pressure) and three internal geological control factors (pore size, water saturation, Specific surface area) on deep CBM and establishes a theoretical model for gas content. Finally, the relationship between the adsorbed gas, free gas, total gas content, and burial depth is calculated using the model, uncovering the primary factors controlling the occurrence state of deep CBM. This research is of significant importance in providing key parameters for gas content in deep coal and optimizing deep CBM exploration.

KEYWORDS

deep coalbed methane, occurrence state, controlling factors, simplified local density model, molecular simulation

1 Introduction

China possesses abundant CBM resources, particularly in deep coal seams. CBM resources with depths exceeding 1,000 m account for 63% of the total proven resources (Geng et al., 2018). However, the exploration of deep CBM poses significant challenges, and the theoretical foundation for its development is relatively weak. There is insufficient understanding of the key controlling factors of the occurrence state of deep CBM. Deep CBM primarily exists in the coal matrix's pore-fracture system in the forms of adsorbed gas, free gas, and dissolved gas (Yao et al., 2014; Liu et al., 2018; Li et al., 2022). Therefore, it is

crucial to identify the primary controlling factors of the occurrence state of deep CBM for the optimal selection of sweet spots in deep CBM development.

Deep CBM reservoirs exhibit significant high-temperature and high-pressure characteristics. Moisture is also commonly present in CBM reservoirs, which can influence the occurrence state of coalbed gas. Furthermore, compared to shallow CBM reservoirs, deep CBM reservoirs are primarily dominated by micropores. Under the combined effects of high temperatures and formation pressures in deep geological formations, microfractures close, porosity decreases, and the heterogeneity of pore structures diminishes (Shen et al., 2014). Over the past few decades, researchers have been studying various controlling factors that impact CBM (Qin and Shen, 2016; Wang and Zhang, 2021; Ye et al., 2021; Tambaria et al., 2022) proposed that in deep CBM reservoirs, the coupling relationship between formation pressure and temperature controls the adsorption characteristics of coal seams as the burial depth increases. Specifically, in shallow depths, the positive effect of pressure on the adsorbed gas content in coal seams is observed. However, as the burial depth increases, the negative effect of temperature on the adsorbed gas content outweighs the positive effect of pressure. Sun et al. (2017) discovered that in the interior of the Baijiahai uplift in the Junggar Basin, deep CBM reservoirs with large, medium, small, and micropores are developed. The coal matrix exhibits strong adsorption energy and can accommodate a considerable amount of adsorbed gas, resulting in the coexistence of adsorbed and free gas reservoirs. Wang et al. (2020) found that moisture has a negative impact on the adsorption characteristics of coal seams. Moisture within the coal occupies methane adsorption sites and blocks the pores. In general, the occurrence state of deep CBM is influenced by factors such as formation temperature, formation pressure, pore structure, and water saturation. Currently, many researchers have studied the impact of specific controlling factors on deep CBM through experimental methods (Wang et al., 2020). However, due to the heterogeneity of experimental samples and limitations of the experimental methods, it is challenging to quantitatively characterize the influence of various controlling factors on the occurrence state of deep CBM using experimental approaches.

In recent years, with the advancement of numerical simulation methods, various theoretical approaches have been developed to study the adsorption characteristics of CBM, such as the Simplified Local Density (SLD) model (Qi et al., 2019; Huang et al., 2022; Pang et al., 2022), molecular simulation (Meng et al., 2018; Bai et al., 2021), and density functional theory (Yan and Yang, 2005). The SLD model, proposed by Rangarajan et al. (1995), considers that the adsorption effect is jointly influenced by the fluid-fluid interactions among adsorbate molecules and the fluid-solid interactions between adsorbate molecules and the adsorbent. To improve the accuracy of the model under high pressures, (Fitzgerald et al., 2003) introduced an empirical parameter to correct the excess volume parameter. With this modification, the SLD model has been widely used to investigate gas adsorption behavior in porous media.

Many researchers have successfully applied molecular simulation methods to investigate the distribution of methane molecules in different pore structures and the influence of various controlling factors, such as water saturation, on the occurrence state of CBM (Zhang et al., 2017; Hao et al., 2022; Yao et al., 2023).

Although researchers have made significant explorations using SLD model or molecular simulation methods to study the occurrence state of coalbed methane, these individual methods still have some limitations when studying the influence of different controlling factors on the occurrence state of coalbed methane. For example, the SLD model cannot accurately characterize the distribution of methane in different coal pore structures and the effect of water saturation, which are important external controlling factors on the occurrence state of coalbed methane. Molecular simulation methods involve complex calculations and idealized microscopic conditions, which may not be applicable at a macroscopic level for gas adsorption in coalbeds, as they differ from the actual coalbed environment. Therefore, it is necessary to combine the strengths of both methods to conduct related research and provide a diversified approach for studying the primary controlling factors of the occurrence state of deep coalbed methane.

This study investigated the impact of two external geological controlling factors and two internal geological controlling factors on the occurrence state of deep CBM using the SLD model and molecular simulation, respectively. Subsequently, considering the formation temperature, formation pressure, pore structure, water saturation, and previous research findings, a theoretical model for gas content was established. Finally, based on the theoretical gas content model, the relationship between the adsorbed gas, free gas, total gas content, and burial depth of the coal seam was calculated, and the main controlling factors influencing the occurrence state of deep CBM were discussed. This research provides guidance for determining key parameters of gas content in deep coal seams and optimizing sweet spots for deep CBM.

2 Simulation methodology

2.1 The simplified local density (SLD) model

Rangarajan et al. (1995) proposed a Simplified Local Density (SLD) model by employing the mean-field approximation to simplify the general density functional theory. The SLD model considers that the adsorption effects arise from the collective interactions between adsorbate-adsorbate and adsorbate-adsorbent interfaces. Specifically, the fluid-fluid interactions between adsorbate molecules and the fluid-solid interactions between adsorbate molecules and the adsorbent are assumed to jointly contribute to the adsorption effects. The fluid-fluid interactions between adsorbate molecules are characterized using a gas state equation, while the fluid-solid interactions between adsorbate molecules and the pore walls are described by a potential energy function. As depicted in Figure 1, the SLD model simplifies the pores of the adsorbent into slit-like pores, where an adsorbate molecule located at a distance of z from one pore wall is positioned between the pore walls of a pore with a width of L. The adsorbate molecule experiences collective forces from both pore walls and the remaining adsorbate molecules.

At adsorption equilibrium, the chemical potential of an adsorbate molecule at position z is the sum of the fluid-fluid

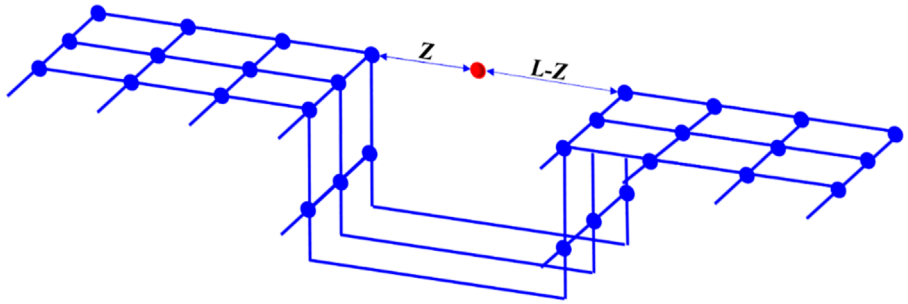

FIGURE 1
The Simplified Local Density (SLD) model.

chemical potential and the fluid-solid chemical potential, and it is equal to the chemical potential in the bulk phase.

$$\mu(z) = \mu_{ff}(z) + \mu_{fs}(z) = \mu_{bulk} \tag{1}$$

Where μ(z) is the chemical potential at the z position in the pore, J·mol^{-1}; z is the distance between the adsorbates and the pore wall, nm; μ_{ff}(z) is the fluid-fluid interaction chemical potential at position z in the pore, J·mol^{-1}; μ_{fs}(z) is the fluid-solid interaction chemical potential at position z in the pore, J·mol^{-1}; μ_{bulk} is the bulk chemical potential in the pore, J·mol^{-1}.

According to thermodynamic equilibrium, chemical potential can be expressed by fugacity in nanopores:

$$\mu_{bulk} = \mu_0(T) + RT\ln\left(\frac{f_{bulk}}{f_0}\right) \tag{2}$$

$$\mu_{ff}(z) = \mu_0(T) + RT\ln\left(\frac{f_{ff}(z)}{f_0}\right) \tag{3}$$

Where μ_0(T) represents any reference state chemical potential, J·mol^{-1}; f_0 refers to the fugacity of any reference state, Pa; f_{bulk} and f_{ff}(z)are respectively the bulk fugacity and the adsorption phase fugacity at z position in the pore, Pa.

In nanopores, the adsorbates are subjected to the force of the pore walls on both sides, and the chemical potential generated can be expressed as follows (Rangarajan et al., 1995):

$$\mu_{fs}(z) = N_A\left[\psi^{fs}(z) + \psi^{fs}(L-z)\right] \tag{4}$$

Where NA is Avogadro's number; Ψ^{fs}(z) and Ψ^{fs}(L-z) are the potential energy generated by the interaction between adsorbates at position z in the pore and the pore walls on both sides, J.

Eqs 2–5 can be obtained simultaneously:

$$f_{ff}(z) = f_{bulk}\exp\left(-\frac{\psi^{fs}(z) + \psi^{fs}(L-z)}{kT}\right) \tag{5}$$

Where k refers to Boltzmann's constant, $1.3806505 \times 10^{-23}$ J K^{-1}.

The fugacity of the bulk phase and the adsorbed phase can be calculated using the Peng-Robinson (PR) equation of state in academic terms (Qi et al., 2019; Huang et al., 2022).

The expression of excess adsorption amount is as follows:

$$n_{ex} = 11.2ZA\int_{lower}^{upper}[\rho(z) - \rho_b]dz \tag{6}$$

Where n_{ex} is the excess adsorption amount, m^3·g^{-1}; A is BET specific surface area, m^2·kg^{-1}; The lower limit and upper limit of the integral are respectively $3/8\sigma_{ff}$ and L-$3/8\sigma_{ff}$; Z is the gas compression factor.

2.2 Molecular simulation methods

Coal is an anisotropic porous material with a complex physicochemical structure, abundant micro- and nano-scale pores, and a high specific surface area, serving as the primary reservoir for CBM. The study area is deep coal in the eastern Ordos Basin. The main coal seam is developed in Taiyuan Formation, numbered 8#, and the coal rank is higher-rank. The molecular structure model of high-rank coal (C184H155O20N3S3) constructed by Wiser et al. (1967) is considered to best reflect the molecular structure of higher-rank coal (Long et al., 2022; Lin et al., 2023). The crystal cell model was established using the Amorphous Cell module and molecular dynamics simulation. Geometric optimization and annealing techniques were employed to achieve global energy minimization of the crystal cell. The optimized cell parameters were a = b = c = 26.77 Å, α = β = γ = 90°. The process of cell construction is illustrated in Figure 2. Subsequently, the cell was expanded to a 1 × 2 × 2 supercell, and a vacuum layer of 5–80 Å was added to obtain the slit model of the coal molecule. The establishment process of the slit model is depicted in Figure 2. It should be noted that in the diagram of methane density distribution in the slit pore, we adopted the center of the pore as the origin, and the distance on both sides of the pore was expressed by positive and negative values, which is a common method to describe the structure and properties of the pore (Mosher et al., 2013; Xiong et al., 2017).

3 Samples and experiments

The samples are deep coal from the eastern Ordos Basin, and the sampling depth is greater than 2000 m. According to various test standards, porosity was measured by helium method, specific surface area and pore diameter were obtained by low temperature CO_2 adsorption experiment and low temperature N_2 adsorption experiment, respectively. The low temperature CO_2 adsorption experiment is to calculate the specific surface area of CO_2 adsorption in coal pores at low temperature (273.15 K) and low pressure. The

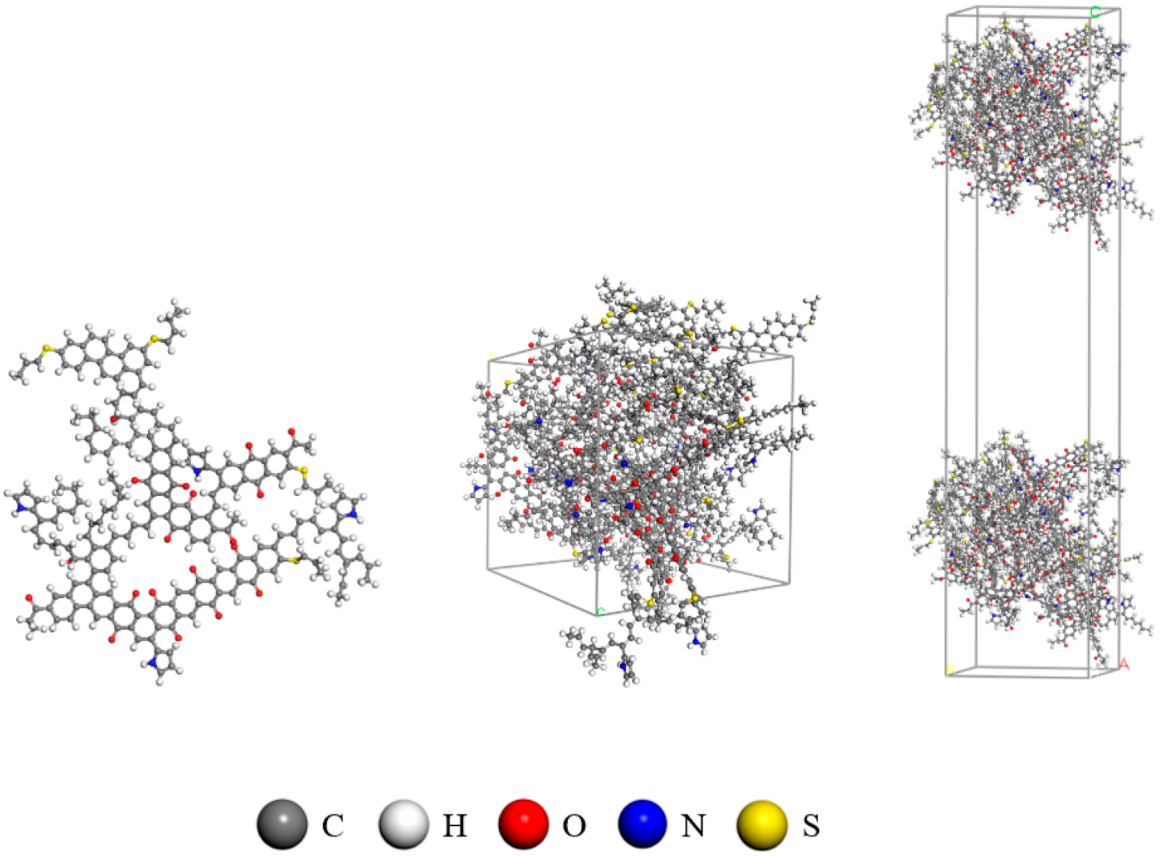

FIGURE 2
Coal molecular matrix model and slit pore model.

TABLE 1 Sample basic data.

Sample	Porosity %	Mad %	Aad %	Vad %	FCad %	BET specific surface area m^2/g	Pore size nm
1	7.9	1.47	3.77	6.43	88.33	78.11	4.97
2	8.9	0.69	9.06	6.55	82.58	112.92	8.62

TABLE 2 Gas content theoretical model parameters.

Porosity	φ = 7%
Water saturation	S_w = 20%
Density	ρ_b = 1.35 g/cm^3
Ground standard temperature	T_{sc} = 30 °C
Temperature gradient	TH = 2.0, 3.0, 4.0 °C/100m
Pressure gradient	PH = 0.85, 0.95, 1.05 MPa/100m

adsorption and desorption curves of N_2 in coal pores under low temperature (77.4 K) and low pressure were used to calculate the pore diameter. BET equation was used to calculate the specific surface area (Brunauer et al., 1938) and BJH equation was used to calculate the pore diameter (Barrett et al., 1951). Table 1 lists the basic information of the samples.

4 Results and discussions

The occurrence state of deep CBM is controlled by various geological factors, which can be broadly categorized into external controlling factors (formation temperature, formation pressure) and internal controlling factors (pore size, water saturation, Specific surface area). In this study, the SLD model is employed to simulate the adsorbed gas content of deep CBM under the influence of both external and internal geological factors. Additionally, molecular simulation methods are utilized to calculate the adsorbed gas and free gas densities under the influence of various controlling factors, as well as their occurrence state within the coal pores.

4.1 External geological controlling factors on the occurrence state of deep CBM

Temperature and pressure are significant external geological controlling factors that influence the content of deep CBM. As

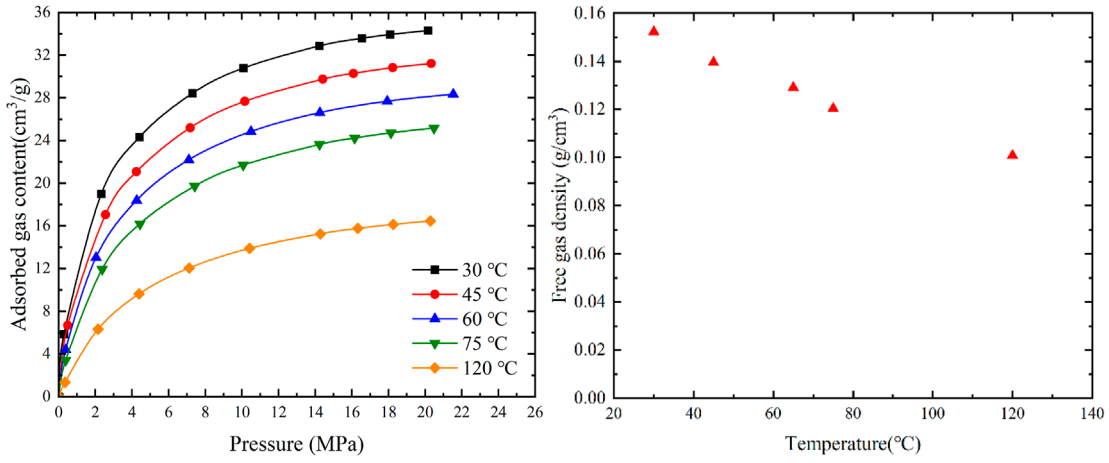

FIGURE 3
The response of gas content in different occurrence states of coal seams to temperature.

the coal seam depth increases, the formation temperature and pressure also increase, leading to a change in the dominant controlling factors for the occurrence state of deep CBM. Consequently, the proportion of adsorbed gas to free gas content is altered.

As shown in Figure 3, when the pressure is 20 MPa and remains unchanged, the adsorbed gas content gradually decreases with increasing temperature. The adsorbed gas content at 120°C is 48% lower than at 30°C. This is due to the physical adsorption of methane, which is an exothermic process. With increasing temperature, the kinetic energy of the adsorbed methane molecules increases, leading to a decrease in the interaction force between methane and the solid surface. Consequently, the adsorption capacity of coal weakens. As shown in Figure 3, at a pressure of 20 MPa, the free gas content also decreases gradually with increasing temperature. The free gas density at 120°C is 31% lower than at 30°C. The influence of temperature on the free gas is relatively smaller compared to the influence on the adsorbed gas.

As shown in Figure 4, the response of Langmuir pressure and Langmuir volume to temperature can be observed. It is evident from the graph that temperature has a negative impact on the adsorption capacity of coal. Both the saturation adsorption capacity exhibit a linear decrease with increasing temperature, showing a high level of linear correlation with good fit (R^2 = 0.9695). In contrast, Langmuir pressure shows a linear increase with temperature, demonstrating a good linear correlation (R^2 = 0.8702). When the temperature increases from 30°C to 120°C, the saturation adsorption capacity decreases from 37.69 cm^3/g to 19.76 cm^3/g, representing a reduction of approximately 47.5%. Meanwhile, Langmuir pressure increases from 2.33 MPa to 5.163 MPa, indicating an approximately 40% increase.

In different injection pressure ranges, the rate of gas content increase can be divided into three stages: rapid, slow, and gradual increase. During the rapid increase stage, CH4 molecules can quickly adsorb onto high-energy adsorption sites. As the high-energy adsorption sites become gradually occupied, the remaining low-energy adsorption sites start adsorbing CH4 molecules, resulting in a slow increase in gas content. Subsequently, as the low-energy adsorption sites become occupied, the adsorption process approaches saturation, and the rate of gas content increase becomes gradual.

As shown in Figure 5, at a constant temperature, the adsorbed gas and free gas content increase with increasing pressure. The adsorbed gas content shows a rapid increase at low pressures and a more gradual increase at high pressures, in accordance with the Langmuir equation. The increase in free gas content within the pore space exhibits a linear trend with increasing pressure, conforming to the gas state equation.

4.2 Internal geological controlling factors on the occurrence state of deep CBM

The deposition of coal and the generation of CBM occur in aqueous environments, and the influence of water content on the gas content and occurrence state of deep CBM cannot be ignored. This section analyzes the distribution of water molecules in coal under different water saturation levels and further investigates the effects of varying water saturation levels on the adsorbed gas and free gas in coal reservoirs.

Coal is an anisotropic porous material with a complex pore structure. The pore structure of coal itself affects the occurrence state of deep CBM. This section analyzes the impact of reservoir pore structure on the occurrence of adsorbed gas and free gas in deep coal reservoirs. By varying pore size and specific surface area, the characteristics of adsorbed gas and free gas content under different pore structure conditions in coal reservoirs are studied.

4.2.1 Water saturation

The distribution of adsorbed water in pores and the interactions among liquid, gas, and solid phases influence the adsorption characteristics of methane molecules in coal. At low water saturation

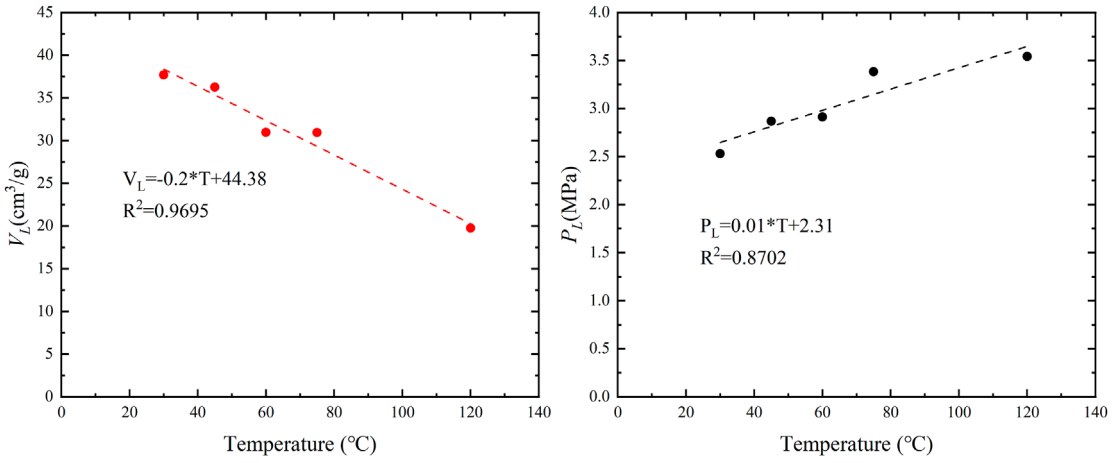

FIGURE 4
The response of Langmuir pressure and Langmuir volume in coal seams to temperature.

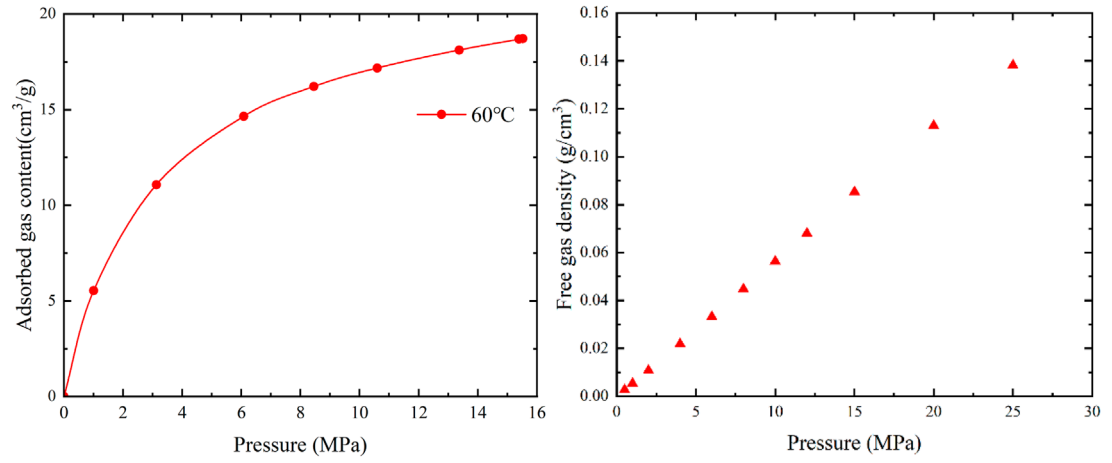

FIGURE 5
The response of gas content in different occurrence states of coal seams to pressure.

levels, there is a "competitive adsorption" relationship between water molecules and methane molecules. However, the adsorption of water molecules on coal is driven by hydrogen bonding between water molecules and pore surfaces, while the adsorption of methane molecules on pore surfaces is driven by van der Waals forces. Hydrogen bonding is 5–10 times stronger than van der Waals forces, causing water molecules to preferentially adsorb and occupy the adsorption sites for methane, resulting in a decrease in the adsorption capacity of methane molecules. As the water saturation level increases, water molecules form a water film on the pore surface and even exhibit capillary condensation in nanometer-sized pores, leading to pore blockage. The formation and thickening of the water film restrict the diffusion pathways of methane molecules.

Figure 6 illustrates the adsorption sites of water and methane molecules within the coal at low water saturation levels. Figure 6 shows the position of methane and water molecules in the Z direction of the model, and the ordinate shows the increase or decrease in the density of methane and water molecules, where the positive value represents the increase in the density of water molecules and the negative value represents the decrease in the density of methane molecules, that is, the methane adsorption site occupied by water molecules. From the figure, it can be observed that water molecules preferentially occupy the micro- and nano-scale pores within the coal, and the density distribution of water molecules in the coal closely corresponds to the reduction in methane molecule density. This indicates a "competitive adsorption" relationship between water and methane molecules, where water molecules have a stronger adsorption capacity on the coal compared to methane molecules.

As shown in Figure 7, with the increase of water saturation, the gas content gradually decreases. For example, when the

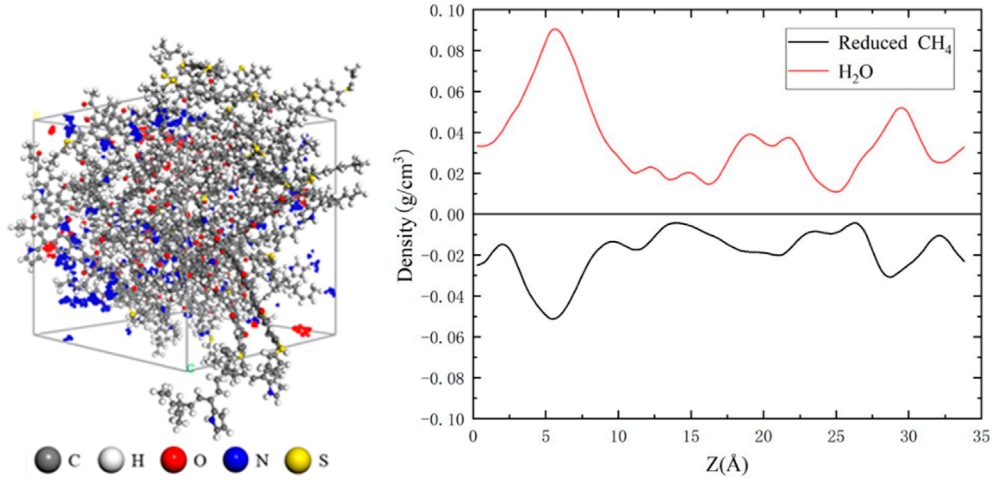

FIGURE 6
Methane reduction and water molecular density distribution.

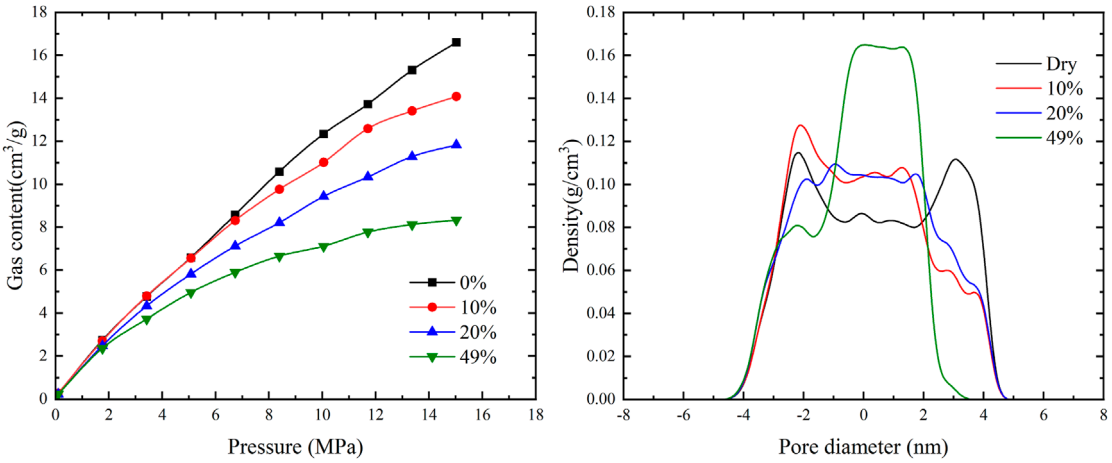

FIGURE 7
The response of gas content in different occurrence states of coal seams to water saturation.

pressure is 15 MPa, the gas content decreases by 49.8% when the water saturation is 49%. This indicates that water saturation has a significant impact on the gas content in coal. The gas density distribution within the pores reveals that water molecules preferentially occupy the adsorption sites of methane molecules. When a water film forms on a single sidewall of a narrow pore, the density distribution curve exhibits a single adsorption peak. However, when water films form on both sidewalls, the adsorption peak disappears, and in a 4 nm pore size, the adsorbed gas and free gas become mixed and indistinguishable.

4.2.2 Pore size

As depicted in Figure 8, when the pore size is less than 2 nm, methane molecules almost completely fill the slit-like pores. As the pore size gradually increases, the density of methane molecules within the pores remains nearly constant. The density of methane molecules in the central region of the pore is similar to that of methane molecules on the pore wall surface, suggesting that methane molecules undergo pore filling phenomena in micropores with a pore size smaller than 2 nm.

As shown in Figure 9, when the pore size is greater than 2 nm, the adsorbed gas density is almost unaffected by the pore size. When the pore size is less than 4 nm, the free gas density is influenced by both sidewalls of the pores, resulting in higher density values. However, when the pore size is larger than 4 nm, the density of free gas is almost unaffected by the pore size, and the density of free gas is lower than the density of methane molecules on the pore wall surface, indicating the absence of pore filling phenomena.

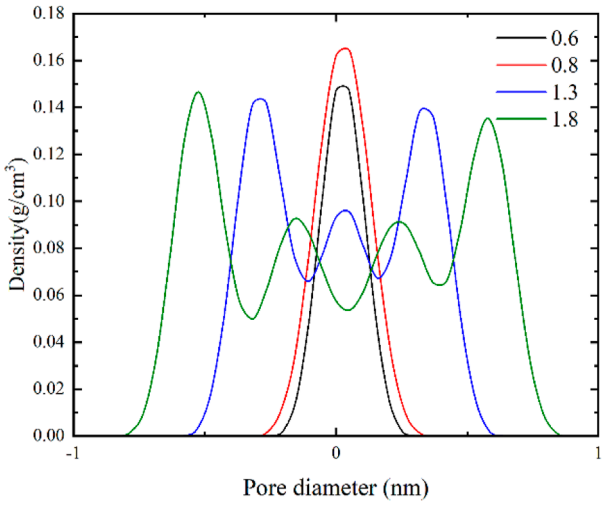

FIGURE 8
Methane density distribution in pores smaller than 2 nm.

Additionally, the methane density distribution for different pore sizes reveals the presence of two adsorption layers on the pore wall surface, suggesting that methane is adsorbed in a multi-molecular layer form in pores larger than 2 nm. The results of the gas content for different pore sizes show adsorption reversal phenomenon at high pressures. At low pressures, due to the smaller pore size and stronger binding energy within the small pores, methane molecules preferentially adsorb, resulting in a higher gas content in models with larger pore sizes. As the pressure increases, the adsorption sites in the small pores become occupied, leading to a slower increase in the adsorbed gas content and resulting in a phenomenon where the gas content in larger pores is greater than that in smaller pores.

4.2.3 Specific surface area

The CO_2 adsorption experiments provide insights into the specific surface area, pore volume, and adsorption capacity characteristics of micropores with sizes below 2 nm. The specific surface area of coal in the local area was measured in the range of 65.76 to 135.29 m^2/g, with an average of 106.86 m^2/g. Based on these measurements, four theoretical conditions were set at 65, 85, 100, and 120 m^2/g to analyze the impact of specific surface area on the adsorbed gas and free gas in coal.

As depicted in Figure 10, increasing the specific surface area does not alter the density of adsorbed gas and free gas. However, it provides more adsorption sites for methane adsorption. At 120 m^2/g, the gas content of adsorbed gas is four times higher than that at 65 m^2/g, indicating that a larger specific surface area leads to higher gas content in terms of adsorbed gas. The change in specific surface area has little impact on the content of free gas because free gas primarily exists in pores and fractures without interacting with the pore walls.

4.3 Theoretical model of gas content

As mentioned in the previous section, the gas content of coal seams is primarily controlled by the specific surface area, water saturation, formation temperature, and formation pressure of the coal seam. By integrating coal seam temperature, pressure, industrial components of coal, rock physics experiments, and relevant research findings from domestic and international sources, a theoretical model for the gas content of deep coal adsorption is established.

$$n_{ex} = 11.2ZA\int_{lower}^{upper}[\rho(z) - \rho_b]dz \tag{7}$$

In the model, the potential energy of solid-solid interactions (ε_{ss}) is found to be a function of temperature and water saturation. Through research investigations, it has been determined that in deep coal, ε_{ss} exhibits the following functional relationship with temperature and other conditions (Zeng, 2019).

$$\begin{aligned}\varepsilon_{ss}/k_B = &\left[(-0.0081V_{ad} + 0.55)(T - 308.15) + 0.39FC_{ad} + 3.67\right] \\ &\times\left[1 + 0073(M_{EMC} - S_w)\right]\end{aligned} \tag{8}$$

In the equation, A_{ad} represents the ash content, %. FC_{ad} represents the fixed carbon content, %. M_{ad} represents the moisture content, %. V_{ad} represents the volatile matter content, %. M_{EMC} represents the equilibrium moisture content, %. S_w represents the water saturation, %.

Free gas is primarily stored in coal seam pores and microfractures. Through analysis of internal and external geological controlling factors, it is known that the content of free gas is mainly influenced by pore size, water saturation, and temperature-pressure conditions. Since pore size mainly affects the porosity of coal, the content of free gas can be regarded as controlled by porosity, water saturation, geothermal temperature, and formation pressure conditions.

Currently, the calculation of free gas content in unconventional oil and gas reservoirs is often based on gas state equations and the principle of material balance. Based on previously established models for estimating free gas content, an estimation of the free gas content in deep coal reservoirs is conducted (Eqs 8–10).

$$N_f = \frac{\varphi(1 - S_w)}{\rho_b \cdot B_g} \tag{9}$$

Where, B_g is methane gas volume coefficient.

$$B_g = \frac{P_{sc}ZT}{PT_{sc}} \tag{10}$$

The theoretical model of free gas content in deep coal seam can be obtained by simultaneous upper formula:

$$N_f = \frac{\varphi(1 - S_w)PT_{sc}}{\rho_b P_{sc}ZT} \tag{11}$$

As mentioned earlier, changes in the external geological control factors of temperature and pressure significantly impact the content of adsorbed and free gases in deep coal seams, while the internal geological control factors can be considered constant within the same study area. Based on this, the influence of these two factors on the gas content of coal seams in different occurrence states

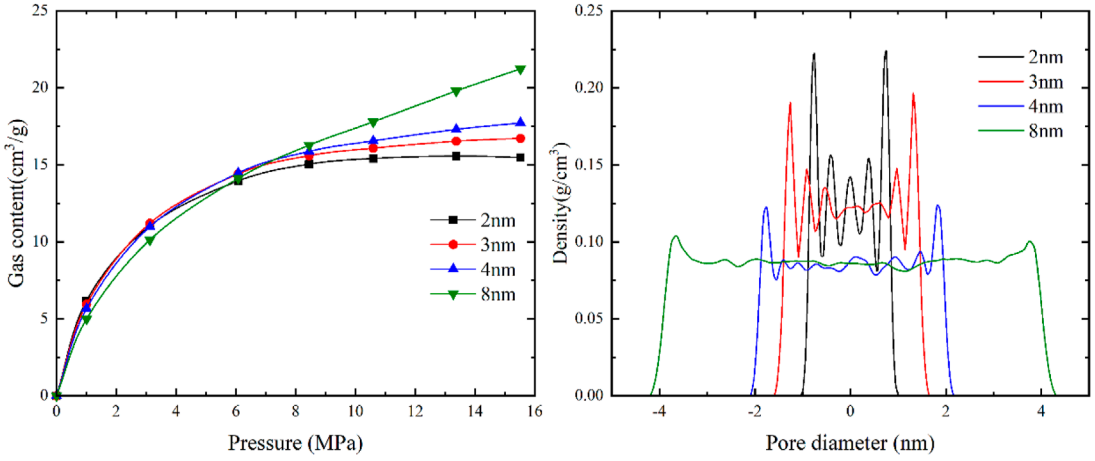

FIGURE 9
The response of gas content in different occurrence states of coal seams to pore size.

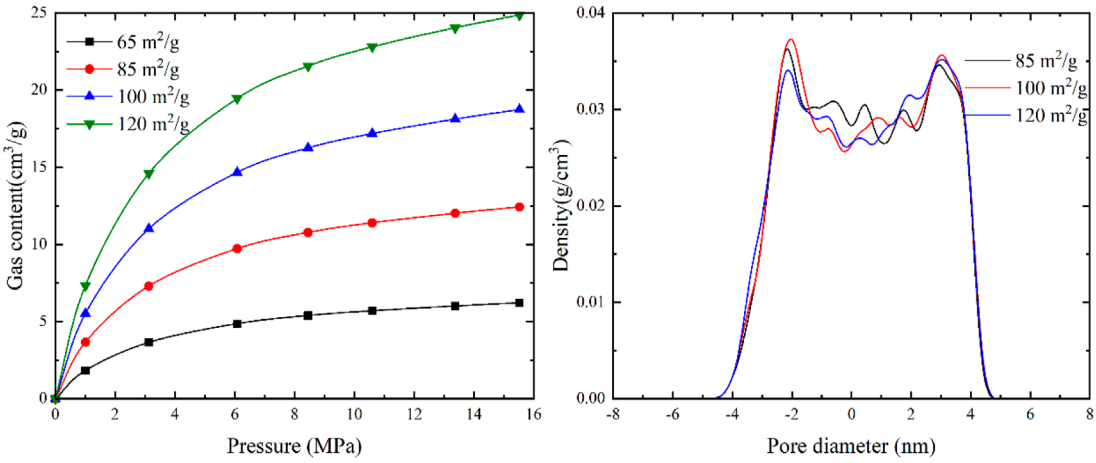

FIGURE 10
The response of gas content in different occurrence states of coal seams to specific surface area.

is discussed. Combined with the formation conditions of deep coalbed methane reservoir in eastern Ordos Basin, three values are assigned to the temperature gradient and pressure gradient, representing the relationship between burial depth and the external geological control factors. The temperature gradient is set to 2.0, 3.0, and 4.0 C/100m, while the pressure gradient is set to 0.85, 0.95, and 1.05 MPa/100 m (Table 2). When one of the two external geological control factors change while keeping the basic parameters constant, the variations in gas content of coal seams in different occurrence states with depth can be obtained by combining Eqs 7, 11 (Figures 11, 12).

With an increase in geothermal gradient, the gas content of adsorbed gas, free gas, and total gas in coal seams continuously decreases (Figure 11). However, the influence of geothermal gradient on adsorbed gas content, free gas content and total gas content of coal seam is different. At shallow layer, the influence of geothermal gradient on adsorbed gas content is weak. With the increase of buried depth, the influence of geothermal gradient on the adsorbed gas content of coal seam increases gradually. The influence of formation temperature on the free gas content of coal seam has the same trend, resulting in the free gas content increasing with the increase of buried depth, but showing a continuous decreasing trend with the increase of geothermal gradient. The total gas content of coal seam is affected by geothermal gradient in the same way as adsorbed gas.

When the ground temperature gradient is unchanged, the adsorbed gas content exhibits a trend of initially increasing and then decreasing, and as the burial depth increases, the differences in adsorbed gas content gradually increase. The maximum adsorbed gas content decreases from 26.8 cm^3/g to 23.01 cm^3/g, corresponding to a decrease in burial depth from 1,291.5 m to 890.2 m. At the same burial depth, the free gas

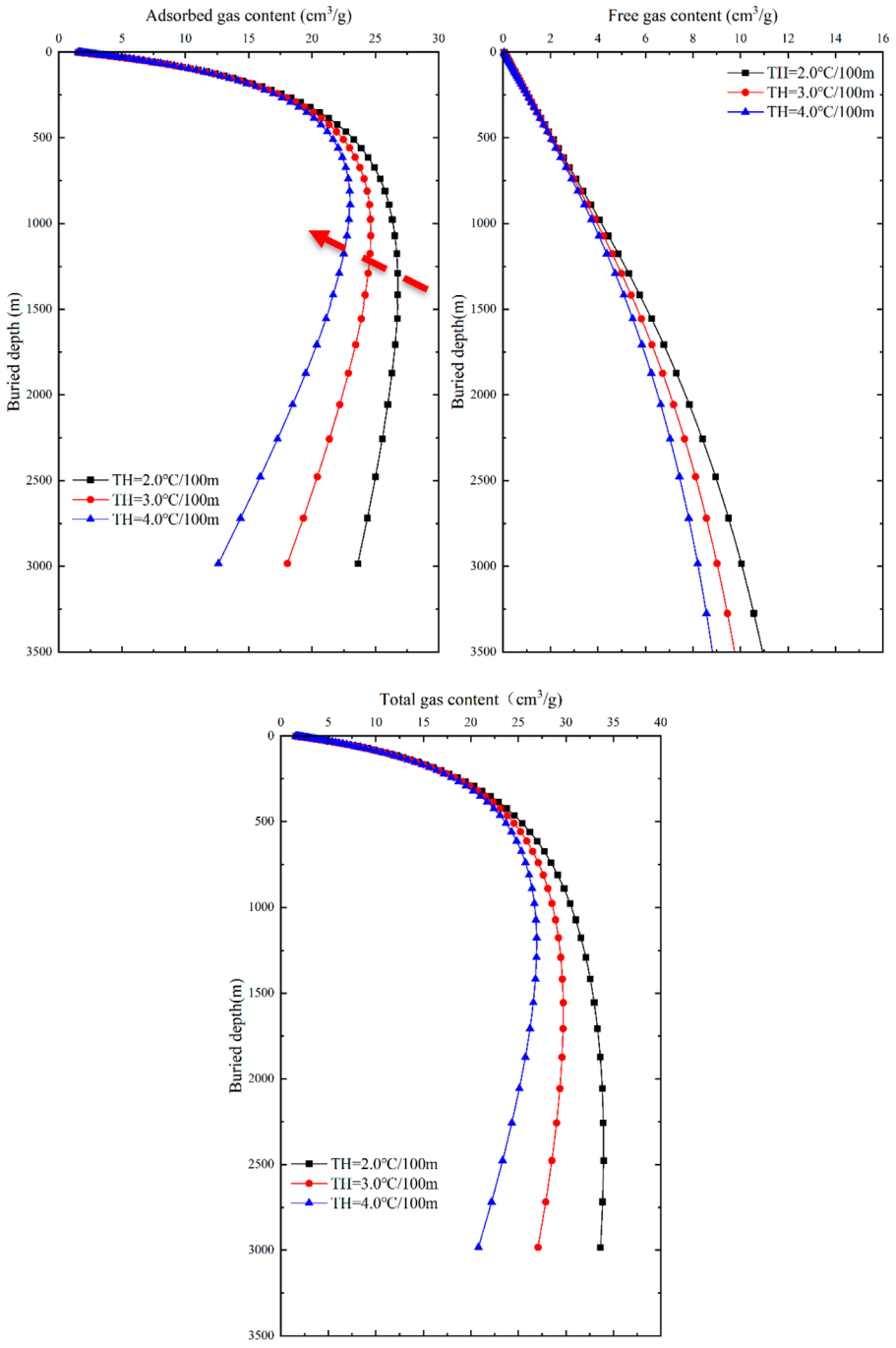

FIGURE 11
Response of gas content and buried depth to temperature in different occurrence states of coal seams.

content in coal seams shows a decreasing trend with an increase in geothermal gradient, and as the burial depth increases, the differences in free gas content also increase. If the burial depth is the constant, the free gas content decreases exponentially with an increase in temperature. The total gas content exhibits a similar response to temperature as the adsorbed gas content, showing a trend of increasing first and then decreasing. The maximum value of total gas content corresponds to a decrease in burial depth from 2477 m to 1,176.8 m.

With an increase in pressure gradient, the gas content of adsorbed gas, free gas, and total gas in coal seams continuously increases, but the differences between the two curves are relatively similar (Figure 12). As the pressure gradient gradually increases, the gas content shows little variation. The adsorbed gas content in coal seams exhibits a trend of initially increasing and then decreasing, with significant differences between 500 m and 1000 m. The maximum adsorbed gas content increases from 24.04 cm^3/g to 25.22 cm^3/g, corresponding to a decrease in burial depth from

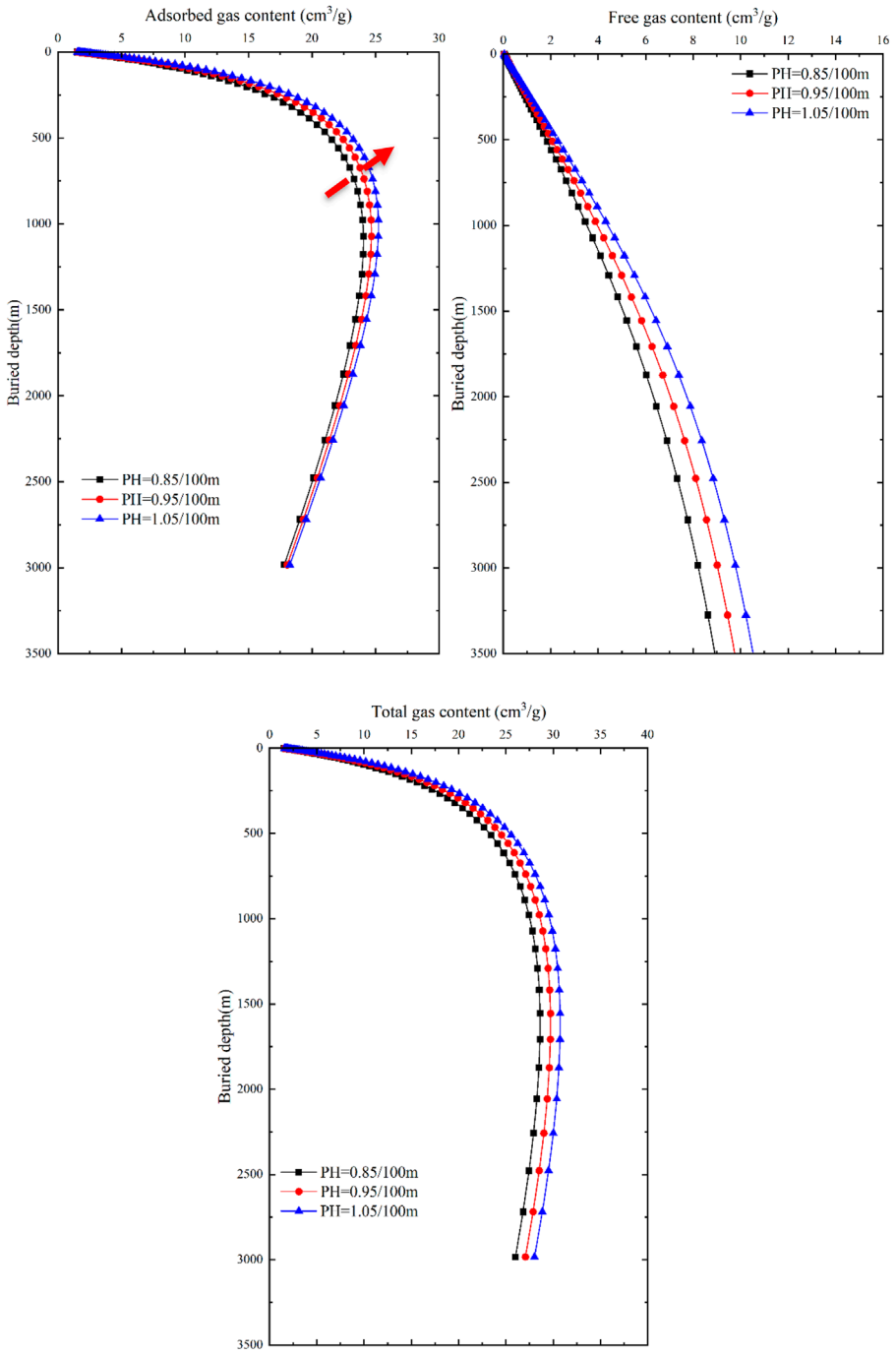

FIGURE 12
Response of gas content and buried depth to pressure in different occurrence states of coal seams.

1,072.3 m to 977 m. As the burial depth continues to increase, the differences in adsorbed gas content gradually decrease, indicating that burial depth is the dominant factor controlling the adsorbed gas content in relatively shallow reservoir depths. As the burial depth increases, temperature becomes the dominant factor controlling the adsorbed gas content. At the same burial depth, the free gas content in coal seams shows an increasing trend with an increase in pressure gradient, and the differences in free gas content remain constant as the burial depth increases. If the burial depth is the same, the free gas content linearly increases with an increase in pressure gradient, indicating that formation pressure plays a dominant role in the free gas content. The total gas content shows slight differences in response to formation pressure compared to the adsorbed gas content, exhibiting a trend of increasing first and then decreasing.

The maximum total gas content is reached at 1555m, but as the burial depth increases, the differences in total gas content gradually approach a constant value.

In the vicinity of 750 m, the impact of geothermal gradient on the total gas content within the tested range approaches that of the pressure gradient. In shallow burial depths (<750 m), there is minimal difference in the total gas content among different geothermal gradients, and all show an increasing trend, indicating that formation temperature is not the dominant factor controlling the total gas content in coal seams. Generally, in shallow burial depths (<750 m), the primary factor influencing the total gas content in coal seams is formation pressure, whereas in deeper burial depths (>750 m), the main factor is formation temperature.

5 A comparison of the primary controlling factors of the occurrence state of deep CBM and shale gas

Shale gas and deep CBM both belong to self-generated and self-stored unconventional natural gas, sharing many similarities in terms of geological conditions and occurrence environments. Factors such as pore structure, temperature, and moisture are also primary controlling factors influencing the occurrence state of shale gas (Gasparik et al., 2014; Merkel et al., 2015; Shabani et al., 2018; Hu et al., 2021; Zhang et al., 2023; Cui et al., 2024). However, there are also some differences between them. Unlike coal, which is primarily composed of organic matter, shale consists not only of organic matter but also of inorganic minerals such as illite and montmorillonite (Shi et al., 2023). In addition to being adsorbed on the surface of organic matter, shale gas can also be adsorbed on the surface of clay minerals. Deep coal and shale also exhibit certain differences in pore structure. Pore structure influences the occurrence state and micro-distribution characteristics of methane (Hu and Cheng, 2023). Shale reservoirs are ultra-tight with diverse pore types, predominantly consisting of micro-nano-scale pores, while coal reservoirs have a dual pore structure composed of pores and fractures, with medium-small pores and micro-pores being dominant, and a wide distribution range of pores. Therefore, further research can compare the influences of mineral composition and pore structure distribution on the occurrence state of deep CBM and shale gas, providing insights into their respective mechanisms.

6 Conclusion

(1) External geological controlling factors, namely temperature and pressure, significantly affect the adsorbed gas and free gas content in deep coal seams. Among the internal geological controlling factors, pore size has a minor impact on the adsorbed gas content, but an increase in pore size leads to larger pore space, providing more accommodation space for free gas and thus having a greater influence on the free gas content. Changes in specific surface area increase the adsorption sites for methane molecules in coal, resulting in an increase in adsorbed gas content, while having no significant effect on the free gas content. The water saturation in coal seams affects both the adsorbed gas and free gas, primarily by occupying the adsorption sites of methane molecules, leading to a decrease in adsorbed gas content, and by forming water films that occupy the reservoir space of free gas as the water saturation increases, resulting in a decrease in free gas content.

(2) In the same study area, there are differences in the influence of geothermal gradient and pressure gradient on the total gas content. The adsorbed gas is predominantly influenced by positive pressure effects in shallow depths and negative temperature effects in deeper depths. The response of free gas to formation pressure is evident under different burial depth conditions, while its response to temperature exhibits exponential decay. In shallow burial depths (<750 m), formation pressure is the primary factor influencing the total gas content in coal seams, whereas in deeper burial depths (>750 m), formation temperature becomes the main influencing factor for the total gas content in coal seams.

Data availability statement

The original contributions presented in the study are included in the article/Supplementary Material, further inquiries can be directed to the corresponding author.

Author contributions

YS: Conceptualization, Data curation, Funding acquisition, Resources, Writing–review and editing. YH: Conceptualization, Funding acquisition, Project administration, Resources, Validation, Writing–review and editing. JW: Investigation, Supervision, Writing–review and editing. JS: Conceptualization, Formal Analysis, Supervision, Writing–original draft. JZ: Software, Supervision, Validation, Visualization, Writing–review and editing. RC: Methodology, Software, Writing–original draft, Writing–review and editing.

Funding

The author(s) declare financial support was received for the research, authorship, and/or publication of this article. The project is supported by CNPC Major Science and Technology Project "Enrichment Law of Deep Coalbed Methane and Optimization of Favorable Areas" (Numbers 2023ZZ18, 2023ZZ1803); China National Petroleum Corporation Logging Co., Ltd. Project "Research on Key Techniques for Logging Evaluation of Deep Coalbed Methane" (Number CNLC2023-8B02).

Conflict of interest

Authors YS, YH, JW, and JZ were employed by China National Logging Corporation.

The remaining authors declare that the research was conducted in the absence of any commercial or financial relationships that could be construed as a potential conflict of interest.

Publisher's note

All claims expressed in this article are solely those of the authors and do not necessarily represent those of their affiliated organizations, or those of the publisher, the editors and the reviewers. Any product that may be evaluated in this article, or claim that may be made by its manufacturer, is not guaranteed or endorsed by the publisher.

Supplementary material

The Supplementary Material for this article can be found online at: https://www.frontiersin.org/articles/10.3389/feart.2024.1340523/full#supplementary-material

References

Bai, Y., Lin, H.-F., Li, S.-G., Yan, M., and Long, H. (2021). Molecular simulation of N2 and CO2 injection into a coal model containing adsorbed methane at different temperatures. *Energy* 219, 119686. doi:10.1016/j.energy.2020.119686

Barrett, E. P., Joyner, L. G., and Halenda, P. P. (1951). The determination of pore volume and area distributions in porous substances. I. Computations from nitrogen isotherms. *J. Am. Chem. Soc.* 73, 373–380. doi:10.1021/ja01145a126

Brunauer, S., Emmett, P. H., and Teller, E. (1938). Adsorption of gases in multimolecular layers. *J. Am. Chem. Soc.* 60, 309–319. doi:10.1021/ja01269a023

Cui, R., Sun, J., Liu, H., Dong, H., and Yan, W. (2024). Pore structure and gas adsorption characteristics in stress-loaded shale on molecular simulation. *Energy* 286, 129658. doi:10.1016/j.energy.2023.129658

Fitzgerald, J., Sudibandriyo, M., Pan, Z., Robinson, R., JR, and Gasem, K. (2003). Modeling the adsorption of pure gases on coals with the SLD model. *Carbon* 41, 2203–2216. doi:10.1016/s0008-6223(03)00202-1

Gasparik, M., Bertier, P., Gensterblum, Y., Ghanizadeh, A., Krooss, B. M., and Littke, R. (2014). Geological controls on the methane storage capacity in organic-rich shales. *Int. J. Coal Geol.* 123, 34–51. doi:10.1016/j.coal.2013.06.010

Geng, M., Chen, H., Chen, Y., Zeng, L., Chen, S., and Jiang, X. (2018). Methods and results of the fourth round national CBM resource evaluation. *Coal Sci. Technol.* 46, 64–68. doi:10.13199/j.cnki.cst.2018.06.011

Guo, T. (2022). Prediction model of occurrence and content of deep coalbed methane. Master Thesis. China: China University of Mining and Technology.

Hao, M., Wei, C., and Zhang, H. (2022). Adsorption and diffusion of methane in coal slit pores: insights into the molecular level. *Energy & Fuels* 36, 880–886. doi:10.1021/acs.energyfuels.1c03730

Huang, X., Gu, L., Li, S., Du, Y., and Liu, Y. (2022). Absolute adsorption of light hydrocarbons on organic-rich shale: an efficient determination method. *Fuel* 308, 121998. doi:10.1016/j.fuel.2021.121998

Hu, B., Cheng, Y., and Pan, Z. (2023). Classification methods of pore structures in coal: a review and new insight. *Gas Sci. Eng.* 110, 204876. doi:10.1016/j.jgsce.2023.204876

Hu, Z., Gaus, G., Seemann, T., Zhang, Q., Littke, R., and Fink, R. (2021). Pore structure and sorption capacity investigations of Ediacaran and Lower Silurian gas shales from the Upper Yangtze platform, China. *Geomechanics Geophys. Geo-Energy Geo-Resources* 7, 71. doi:10.1007/s40948-021-00262-5

Lin, H.-F., Long, H., Li, S.-G., Bai, Y., Xiao, T., and Qin, A.-L. (2023). CH4 adsorption and diffusion characteristics in stress-loaded coal based on molecular simulation. *Fuel* 333, 126478. doi:10.1016/j.fuel.2022.126478

Liu, S., Tang, S., and Yin, S. (2018). Coalbed methane recovery from multilateral horizontal wells in Southern Qinshui Basin. *Adv. Geo-Energy Res.* 2, 34–42. doi:10.26804/ager.2018.01.03

Li, Y., Wang, Z., Tang, S., and Elsworth, D. (2022). Re-evaluating adsorbed and free methane content in coal and its ad-and desorption processes analysis. *Chem. Eng. J.* 428, 131946. doi:10.1016/j.cej.2021.131946

Long, H., Lin, H.-F., Li, S.-G., Bai, Y., Qin, L., Xiao, T., et al. (2022). Nanomechanical properties of CH4-containing coal during CO2 storage under different injection pressures based on molecule dynamics. *Appl. Surf. Sci.* 590, 153126. doi:10.1016/j.apsusc.2022.153126

Meng, J., Zhong, R., Li, S., Yin, F., and Nie, B. (2018). Molecular model construction and study of gas adsorption of Zhaozhuang coal. *Energy & Fuels* 32, 9727–9737. doi:10.1021/acs.energyfuels.8b01940

Merkel, A., Fink, R., and Littke, R. (2015). The role of pre-adsorbed water on methane sorption capacity of Bossier and Haynesville shales. *Int. J. Coal Geol.* 147, 1–8. doi:10.1016/j.coal.2015.06.003

Mosher, K., He, J., Liu, Y., Rupp, E., and Wilcox, J. (2013). Molecular simulation of methane adsorption in micro-and mesoporous carbons with applications to coal and gas shale systems. *Int. J. Coal Geol.* 109, 36–44. doi:10.1016/j.coal.2013.01.001

Pang, Y., Wang, S., Yao, X., Hu, X., and Chen, S. (2022). Evaluation of gas adsorption in nanoporous shale by simplified local density model integrated with pore structure and pore size distribution. *Langmuir* 38, 3641–3655. doi:10.1021/acs.langmuir.1c02408

Qin, Y., and Shen, J. (2016). On the fundamental issues of deep coalbed methane geology. *Acta Pet. Sin.* 37, 125.

Qi, R., Ning, Z., Wang, Q., Huang, L., Wu, X., Cheng, Z., et al. (2019). Measurements and modeling of high-pressure adsorption of CH4 and CO2 on shales. *Fuel* 242, 728–743. doi:10.1016/j.fuel.2018.12.086

Rangarajan, B., Lira, C. T., and Subramanian, R. (1995). Simplified local density model for adsorption over large pressure ranges. *AIChE J.* 41, 838–845. doi:10.1002/aic.690410411

Shabani, M., Moallemi, S. A., Krooss, B. M., Amann-Hildenbrand, A., Zamani-Pozveh, Z., Ghalavand, H., et al. (2018). Methane sorption and storage characteristics of organic-rich carbonaceous rocks, Lurestan province, southwest Iran. *Int. J. Coal Geol.* 186, 51–64. doi:10.1016/j.coal.2017.12.005

Shen, J., Qin, Y., Fu, X., Chen, G., and Chen, R. (2014). Properties of deep coalbed methane reservoir-forming conditions and critical depth discussion. *Nat. Gas. Geosci.* 25, 1470–1476.

Shi, K.-Y., Chen, J.-Q., Pang, X.-Q., Jiang, F.-J., Hui, S.-S., Zhao, Z.-C., et al. (2023). Wettability of different clay mineral surfaces in shale: implications from molecular dynamics simulations. *Petroleum Sci.* 20, 689–704. doi:10.1016/j.petsci.2023.02.001

Sun, B., Yang, M., and Yang, Q. (2017). Analysis on occurrence state of deep coalbed methane in Junggar basin. *J. China Coal Soc.* 42, 195–202.

Tambaria, T. N., Sugai, Y., and Nguele, R. (2022). Adsorption factors in enhanced coal bed methane recovery: a review. *Gases* 2, 1–21. doi:10.3390/gases2010001

Wang, W.-S., and Zhang, J.-J. (2021). Study on the driving factors and regulation mode for coal production capacity. *Petroleum Sci.* 18, 1564–1577. doi:10.1016/j.petsci.2021.08.014

Wang, F., Yao, Y., Wen, Z., Sun, Q., and Yuan, X. (2020). Effect of water occurrences on methane adsorption capacity of coal: a comparison between bituminous coal and anthracite coal. *Fuel* 266, 117102. doi:10.1016/j.fuel.2020.117102

Wiser, W., Hill, G., and Kertamus, N. (1967). Kinetic study of pyrolysis of high volatile bituminous coal. *Industrial Eng. Chem. Process Des. Dev.* 6, 133–138. doi:10.1021/i260021a023

Xiong, J., Liu, X., Liang, L., and Zeng, Q. (2017). Adsorption of methane in organic-rich shale nanopores: an experimental and molecular simulation study. *Fuel* 200, 299–315. doi:10.1016/j.fuel.2017.03.083

Yan, B., and Yang, X. (2005). Adsorption prediction for three binary supercritical gas mixtures on activated carbon based on a NDFT/PSD approach. *Chem. Eng. Sci.* 60, 3267–3277. doi:10.1016/j.ces.2005.01.035

Yao, Y., Liu, D., and Xie, S. (2014). Quantitative characterization of methane adsorption on coal using a low-field NMR relaxation method. *Int. J. Coal Geol.* 131, 32–40. doi:10.1016/j.coal.2014.06.001

Yao, Y., Zhang, C., Ye, S., Sun, X., and Wu, H. (2023). Water-methane interactions in coal: insights from molecular simulation. *Unconv. Resour.* 3, 113–122. doi:10.1016/j.uncres.2023.01.004

Ye, D., Liu, G., Gao, F., Xu, R., and Yue, F. (2021). A multi-field coupling model of gas flow in fractured coal seam. *Adv. Geo-Energy Res.* 5, 104–118. doi:10.46690/ager.2021.01.10

Zeng, Q. (2019). Experiment and modeling studies on coalbed methane recovery mechanism in deep coal seams. Doctor thesis. Beijing: China University of Petroleum.

Zhang, Q., Fink, R., Krooss, B. M., Jin, Z., Zhu, R., Hu, Z., et al. (2023). Effects of light hydrocarbons and extractable organic matter on the methane sorption capacity of shales. *AAPG Bull.* 20, 230–801 doi:10.1306/05302322009

Zhang, T., He, Y., Yang, Y., and Wu, K. (2017). Molecular simulation of shale gas adsorption in organic-matter nanopore. *J. Nat. Gas Geoscience* 2, 323–332. doi:10.1016/j.jnggs.2018.01.001